Int J Adv Manuf Technol (2014) 75:1773–1786
DOI 10.1007/s00170-014-6271-z

ORIGINAL ARTICLE

# Investigating the effect of WEDM process parameters on 3D micron-scale surface topography related to fractal dimension

**Guofu Luo · Wuyi Ming · Zhen Zhang · Min Liu · He Li · Yihao Li · Ling Yin**

Received: 11 July 2013 / Accepted: 10 August 2014 / Published online: 30 August 2014


**Abstract** The wire electric discharge machining (WEDM) process is a violent thermal process in which a certain volume of metal is eroded by thousands of electrical discharges in a fraction of 1 s. The process is widely used in tooling, especially in the cutlery and mold industry. However, the poor properties of surfaces such as high tensile residual stresses, high surface roughness, white layers, and microcracks are generated in the process. These properties vary with different levels of process parameters. In this paper, a new graphical evaluation of micron-scale surface topography on WEDM process is proposed by the fractal method. The objective is to quantify 3D micron-scale surface topography effect of process parameters such as pulse-on time, pulse-off time, cutting feed rate, wire tension, wire speed, and water pressure on working surface in dressing. Firstly, adaptive measuring was conducted on the basis of 3D micron-scale surface topography by the $Ł_{18}(2^1 \times 3^5)$ Taguchi standard orthogonal experiments; secondly, the fractal dimension was conducted to identify 3D micron-scale surface topography; and finally, the effect of WEDM process parameters was investigated with reference to the fractal dimension (FD) of 3D micron-scale surface. The results have shown that the pulse-on time is the most dominant factor in affecting the surface texture. Moreover, the interaction effect between process parameters is analyzed. It has also been observed that the optimized combination of pulse-on time of 3 μs, pulse-off time of 20 μs, cutting feed rate of 4 mm/min, wire tension of 6 kgf, wire speed of 6 m/min, and water pressure of 5 kgf is suitable for 3D micron-scale surface, and the FD of 3D micron-scale surface is increased by 11 %.

**Keywords** WEDM · 3D surface topography · Fractal dimension · Taguchi orthogonal array · Optimization

## 1 Introduction

Nonconventional machining processes such as the wire electric discharge machining (WEDM) are being widely used in machine hard tool and die materials used in the industries. WEDM is a process whereby the process removes the workpiece material by a series of electrical sparks, which generate discharge craters and recast layers on the surface of the workpiece, between the wire electrode and the workpiece. The mechanical, metallurgical, topological, and chemical conditions of the surface region are described in the surface integrity. Then, a comprehensive description of the surface integrity on the WEDM surface involves the measurement of surface roughness, depth of the heat-affected zone, microhardness, size of the surface crater, and residual stresses [1]. Yang et al. [2] visualized the forming process of discharge craters in three dimensions with relatively small discharge energy and clarified the mechanism of material removal and formation of discharge

G. Luo · W. Ming · Y. Li
Department of Electromechanical Science and Engineering, Zhengzhou University of Light Industry, 450002 Zhengzhou, China
e-mail: luogufu@zzuli.edu.cn

L. Yin (✉)
School of Mechanical Engineering, DongGuan University of Technology, 523808 Dongguan, China
e-mail: yinling78@163.com

Z. Zhang · M. Liu · H. Li
School of Mechanical Science and Engineering, Huazhong University of Science and Technology, 430074, Wuhan, China

crater shapes. Qu et al. [3] evaluated the surface integrity and roundness of cylindrical WEDM parts by proposing a mathematical model, which investigated the surface integrity and roundness of WEDM parts and explored one way to optimize process parameters in order to achieve better surface integrity and roundness. Some investigations have been carried out in order to analyze and improve the surface integrity of workpieces created by WEDM. They studied the effects of machining settings on the behavior of pulse trains for tool steels [4] and the cutting mechanisms for metal matrix ceramic composites [5], and they found that the surface roughness (Ra) of the WEDM-processed workpiece was about 0.2 to 0.4 μm for tool steels and 1.4 to 3.9 μm for metal matrix ceramic composites. A new approach, which changes the normal machining conditions, was put forward by Aminollah et al. [6] to improve surface roughness for turning WEDM. Ramakrishnan and Karunamoorthy [7] established mathematical models, which used the Gauss elimination method for the WEDM machining, relating to the machining performance in order to analyze and improve the surface roughness. Taguchi's robust design approach was proposed for the WEDM or EDM operation in order to optimize the MRR and surface roughness (Ra) [8–10]. Mohammadi et al. [8] and Huang et al. [10] also used Taguchi's method with ANOVA to study the relationship between WEDM input and output measures. The artificial neural network [11–13] was also utilized to establish a mathematical relationship between the machining parameters and output measures. In addition, the artificial neural network was also used in other manufacturing fields [14, 15]. It can be seen from above that the characteristics of the surface integrity of workpieces are mostly described in two dimensions to optimize the WEDM cutting conditions. However, there are few investigations on micron-scale surface in WEDM. Ramasawmy and Blunt [16] studied that 3D surface parameters was used as a basis to characterize the surface produced by the combined processes in different electrolytic media and that 3D surface characterization was carried out in order to calculate the different surface texture parameters in EDM process [17] . In addition, there is a lack of a global index evaluation on characterization of 3D micron-scale surface topography, especially in WEDM process. Many machined surfaces such as those processed by turning, electrical discharging machining, grinding, and rubbing, which have the property of self-similarity or self-affinity, can be characterized with fractal geometry. Jian et al. [18] proposed a concise method based on 2D Fourier transform to compute the surface fractal dimension (FD) and to analyze the anisotropy along 3D machined surfaces. Chen et al. [19] analyzed the 3D microtopography in machined potassium dihydrogen phosphate crystal surfaces based on fractal and wavelet methods. However, there have been few detailed research reports on the structural figures of 3D micron-scale surface topography. The reason for this is that they have complex fractal features and the traditional linear methodologies do not work for studying them. With the development of fractal theory [20], it has been ascertained that most of natural objects and their images have spatial fractal characteristics, and the shape information of an object can be obtained by means of the characteristics of its images. In engineering application, a novel method based on fractal geometry [21] for visual analysis and classification of operational sequences was proposed to improve manufacturing quality. In medical application, a tissue characterization method was proposed for coronary plaques by using fractal analysis-based features [22]. In this paper, a new graphical evaluation of micron-scale surface topography in WEDM process is proposed by fractal dimension. The objective is to quantify 3D micron-scale surface topography effect of process parameters such as pulse-on time, pulse-off time, cutting feed rate, wire tension, wire speed, and water pressure on working surface in dressing. Firstly, adaptive measuring was conducted on the base of 3D micron-scale surface topography by the $Ł_{18}(2^1 \times 3^5)$ Taguchi standard orthogonal experiments; secondly, the FD was conducted to identify 3D micron-scale surface topography; and finally, the effect of WEDM process parameters was investigated with reference to the FD of 3D micron-scale surface.

## 2 Estimation of FD

### 2.1 Concept of fractal

Mandelbrot [23] defined FD as a set for which the Hausdorff dimension (Dh) is greater than its topological dimension. Self-similarity is one criterion of a FD. It can be explained as follows: Considering a bounded set $A$ in Euclidean $n$-space, the set is said to be self-similar when $A$ is the union of $N_r$, distinct (nonoverlapping) copies of itself, and each of which is similar to $A$ scaled down by a ratio $r$. The FD of $A$ can be drawn from the relation in Eq. 1, where $D$ is the FD.

$$D = \frac{\log(N_r)}{\log(1/r)} \tag{1}$$

It has been known that the profile $Z(x, y)$ of machining surface appears multiscale, random, and disordered in precision machine. The mathematical properties of the profile are not differentiable, continuous, and statistically

self-affine. It was found that all these properties are satisfied by Weierstrass-Mandelbrot (W-M) function [24], which is given as follows:

$$Z(x,y) = A \times \sum_{n1,n2=0}^{\infty} a_{n1,n2} \frac{\gamma(n1+n2)^2}{[\gamma^{2n1}+\gamma^{2n2}]^{(4-D_s)^2}} \times \cos(2\pi\gamma^{n1}x + \theta_{n1,n2}) \times \cos(2\pi\gamma^{n2}y + \phi_{n1,n2}) \quad (2)$$

where the parameter $D_s$ is the FD; $\theta$ and $\phi$ are the random phase between 0 and 2; $A$ is a characteristic length scale of the surface; and $\gamma^n$ determines the frequency spectrum of the machining surface roughness.

### 2.2 Concept of BC method

The box-counting (BC) method, which is defined by Russel et al. [25], is the most frequently used and popular method. There is a series equivalent definition about box-counting dimension, including grid overlay method. Taking into account the image stored in a computer by the size of $M \times M$ pixels (2D) or $M \times M \times M$ pixels (3D), the box-counting dimension calculation of the binary image is also known as pixel coverage method. The BC method consists of three major steps: (1) meshing the grid image using different step sizes, (2) counting the number of boxes that contain the object of interest, and (3) performing least-squares regression of log $(N_r)$ versus log $(1/r)$ in order to obtain the FD by the slope of the fitted line. Detailed descriptions are listed below. The BC algorithm requires that the image is binary. Consider that the 3D binary image (only having white and black color) of size $M \times M \times M$ pixels has been scaled down to a size $s \times s \times s$ is an integer. Then the scaling ratio becomes $r = s/M$. After this, the image is partitioned into $M/s \times M/s \times M/s$ grids. Each grid containing pixels of the region of interest (white or black object) is considered to be an occupied (or countable) grid. Subpanels a, b, c, and d of Fig. 1 contain one, two, four, and eight black objects, respectively. When the number of black objects is greater than the $p$ which is the key parameter of the BC algorithm, the grid is considered to be countable. The total number of those grids is counted as $N_r$. This process is repeated for grids with different sizes of $s$ (i.e., $r$), and different $N_r$ will be obtained. Then FD is calculated as the slope of the fitted linear regression curve of the log $(N_r)$ against log $(1/r)$ with Eq. 1. The procedure which is listed in Table 1 is implemented on MATLAB 7.10 R2010a.

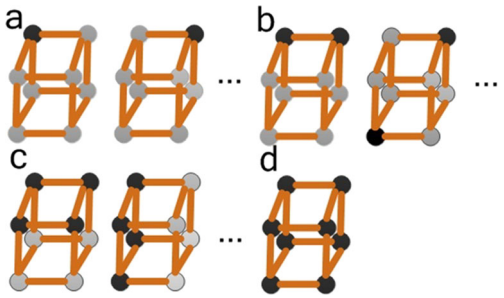


**Fig. 1** The interest of one grid: **a** one black object, **b** two black objects, **c** four black objects, and **d** eight black objects

## 3 Experiment, 3D measurement, and construction of 3D surface topography

This section includes three subsections. Firstly, the WEDM experiment were done by the $Ł_{18}(2^1 \times 3^5)$ Taguchi standard orthogonal array. Secondly, the micron-scale surface topography of YG15 workpiece was measured by 3D white light interferometer measurement. Finally, the method of construction of 3D surface topography was proposed. The analysis of 3D micron-scale surface topography and the optimized parameters of WEDM are shown in the next section. Figure 2 illustrates the procedures implemented in this research.

### 3.1 WEDM experiment

In this research, the WEDM machining experiment was done by W-A530 WEDM machine, which is made by Dongguan Hustinova Precision Machinery Co., Ltd. Figure 3 shows the experimental equipment. The WEDM machine is equipped with anti-electrolysis plus generator, of which average voltage is zero to prevent oxidation of the material of the workpiece.

The workpiece is a 40-mm-thick block of YG15 steel (wc, 85 %; co, 15 %). The physical properties of the workpiece are given in Table 2. The cutting brass wire is Cu with a diameter of 0.25 mm. Next, 5-mm-long through cuts are made on the test pieces. The experiment is based on statistical analyses. The Taguchi approach to laying out the experimental conditions significantly reduces the number of tests, overall testing time, and cost of experiments. The experimental data were initially collected based on the Taguchi method of experimental design, which is the $Ł_{18}(2^1 \times 3^5)$ Taguchi standard orthogonal array for machining experiments. The factors and the levels are shown in Table 3. For machining experiments, pulse-on time, pulse-off time, cutting feed rate, wire tension, wire speed, and water pressure are selected as independent variables which

**Table 1** The algorithm process of the box-counting method

| No. | Program | Remark |
|---|---|---|
| Step 1 | Start | |
| | Load 3D binary image | % get the 3D image from one file |
| | Check image size | |
| | [M,M,M] =size(image) | % read the sizes of the image |
| | Select appropriate grid box | |
| | Sizes s(k) | |
| | k=1; | % variable for using different grid box sizes |
| Step 2 | While (s(k) $\leq \log_2(M)$) | |
| | r = s(k)/M; | % define *r* |
| | For i $\leq$ M/s(k),j $\leq$ M/s(k),k $\leq$ M/s(k) | |
| | If the box contains adequate black | % catch the black objects |
| | num =1; | |
| | Else | |
| | num =0; | |
| | End For | |
| | Nr =sum(num); | % count the total number |
| | k = k+1; | % redo for different grid box sizes |
| | End While | |
| Step 3 | Call loglog (1/r, Nr); | % perform linear fit by log-log scale plot |
| | Obtain FD; | % FD equal to the slop of the line |
| | End | |

vary during the rough machining experiments.The settings of these levels cover the commonly used factors for rough cutting in this WEDM. And the second level of three levels is close to the average value of others. Some factors do not change during the experiments, which cannot vary because of the WEDM setup. The pulse discharge current is constant at 10 A in rough cutting, as the setting of pulse discharge current cannot be set in this cutting pattern. These fixed factors are presented in Table 4. In this research, the main effects of factors and its optimization are of interest.

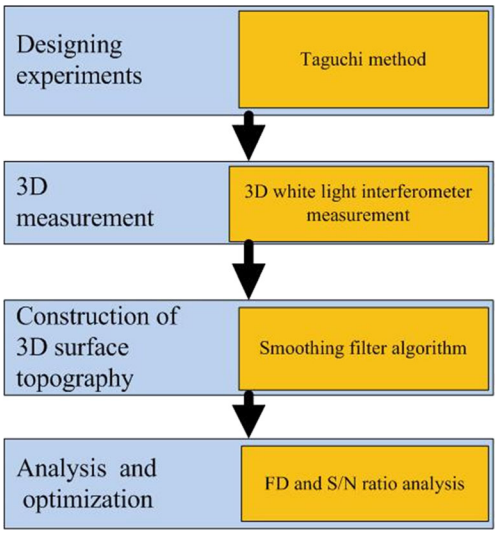


**Fig. 2** The research procedure about 3D micron-scale surface topography on WEDM

## 3.2 3D measurement

Figure 4 shows 3D white light interferometer measurement of YG15 workpiece in WEDM process. In order to study 3D micron-scale surface topography of YG15 workpiece, the 3D white light interferometer measurement (Talysurf CCI 6000, Taylor-Hobson) was employed to measure the workpiece surface by computer auto-measurement system. Both

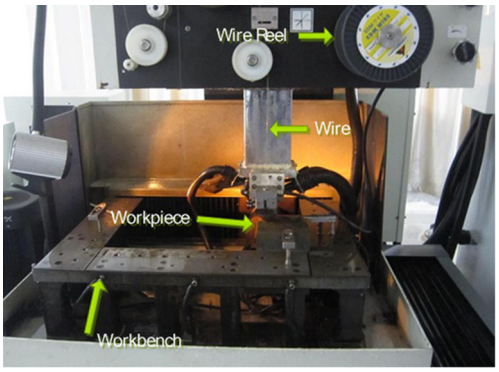


**Fig. 3** Photograph of the experimental equipment

**Table 2** Physical properties of the YG15 steel

| Properties | Value |
|---|---|
| Density (g/cm$^3$) | 13.9 |
| Hardness (HRA) | 87 90 |
| Bending strength (N /mm$^2$) | 2,250 |
| Average particle (nm) | 1.5 |
| Coefficient of expansion (°C$^{-1}$) | $5.3 \times 10^{-6}$ |

$X$-axial and $Y$-axial moving intervals of white light probe were 4 μm, and its vertical feed resolution was 0.5 nm.

### 3.3 Construction of 3D surface topography

There is a lot of noise from the measuring device, the measurement environment, the surface impurities, etc. in the measurement data of the 3D surface topography. For the measured point $Z(i, j)$, the average of its surrounding points $Z_r$ is deemed as follows:

$$Z_r = \frac{1}{(2n_r+1)^2-1}\left(\sum_{m=i-n_r}^{m=i+n_r}\sum_{n=j-n_r}^{m=i+n_r} Z(m,n) - Z(i,j)\right) \tag{3}$$

where $i$ is the point number in $X$-coordinate, $j$ is the point number in $Y$-coordinate, and $n_r$ is the point number around $Z(i, j)$. If $|Z(i, j) - Z_r| \geq e$, then $Z(i, j) = Z_r$, or $Z(i, j)$ is not replaced. The $e$ is used to determine whether the measured point $Z(i, j)$ is a noise. According to the integrity of surface topography on WEDM, the $e$ was chosen as 12 μm in this research. After removing these noises, a smoothing process is needed to be performed, but the contour point of 3D micron-scale surface topography could be destroyed. Hence, contour protection is considered to be valuable. For the measured point $Z(i, j)$, the arithmetic average value $z_s$, which calculates the four measured points around $Z(i, j)$, is drawn as follows:

$$Z_s = \frac{1}{4}\left(\sum_{m=i-1}^{m=i+1} Z(m,j) + \sum_{n=j-1}^{n=j+1} Z(i,n) - 2Z(i,j)\right) \tag{4}$$

The preset threshold value $q$, which determines whether the measured point $Z(i, j)$ should be smoothed, is introduced to protect the surface contour points. If $|Z(i, j) - Z_s| \geq q$, then $Z(i, j) = Z_q$, or $Z(i, j)$ is not replaced. In this research, the $q$ was chosen as 3 μm. Finally, a unified criterion of 3D surface topography needs to be established. Because of the different surface topography of workpieces, there are different average values in each workpiece. Therefore, the revising point $Z_m$ $(i, j)$ is drawn as follows:

$$Z_m = Z(i, j) + \delta \tag{5}$$

where $\delta$ is the revised value which can be fixed in one workpiece and changed in different workpiece. By the revising method, the maximum values of workpieces are the same. Then, the FD of 3D surface topography has a unified criterion. The step of construction of 3D surface topography is depicted as Fig. 5. The measurement area is 1.6 mm × 1.6 mm for all experimental workpieces, and there are three measurement areas per workpiece. The FD of a workpiece is the average value of that three measurement areas. It is obvious that calculation of construction of 3D surface topography is often involved with a large amount of

**Table 4** Fixed factors in the experimentation for machining

| Parameter | Value of the machining |
|---|---|
| Depth of cut (mm) | 0.05 |
| Material | Tool steel YG15 |
| Thickness of specimens (mm) | 40 |
| Workpiece hardness (HRA) | 87∼90 |
| Angle of cut | Vertical |
| Dielectric temperature (°C) | 25 |
| Cutting length (mm) | 10 |
| Power (A) | 10 |

**Table 3** Factors and their level for machining

| Factors | Levels | | |
|---|---|---|---|
| | 1 | 2 | 3 |
| Pulse-on time (μs): time of the discharge pulse duration of high level | 3 | 8 | 13 |
| Pulse-off time (μs): time interval between one discharge and the next | 10 | 20 | 35 |
| Cutting feed rate (mm/min): the maximum setting cutting speed | 1 | 2.5 | 4 |
| Wire tension (kgf): level of mechanical stress | 6 | 10 | 14 |
| Wire speed (m/min): the rate of wire moving | 3 | 4 | 6 |
| Water pressure (kg/cm$^2$): the impact pressure of dielectric flow | 5 | 11 | — |

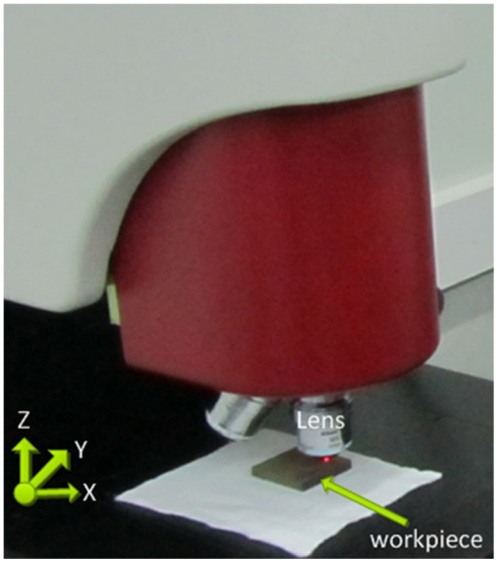


**Fig. 4** 3D white light interferometer measurement of micron-scale surface topography

data. Therefore, it is necessary to work out the result using computer-assisted analysis techniques. In this research, removing the measured noises, smoothing the measured data, and revising data are implemented on MATLAB 7.10 R2010a.

## 4 Result and analysis

### 4.1 3D micron-scale surface topography

It can be seen from Section 2.2 that the different values of $p$ correspond to different FDs. Figure 6 shows the FD on the different values of $p(= 1, 2, 4, 8)$ in two samples in which the experiment numbers are 2 and 6 (see Table 5). When $p$ is 1, 2, 4, and 8, the difference of FD in two samples is 0.0772, 0.0366, 0.0381, and 0.0302, respectively. The difference of FD is greater, and the discriminative of 3D micron-scale surface topography is better. Therefore, in this paper, the $p$ is to set 1, and the FD calculated below is based on this setting.

The different FD of 3D micron-scale surface topography for each of the 18 samples were calculated from the data collected by the 3D white light interferometer measuring equipment. Table 5 shows the machining response data acquired for FD by the $Ł_{18}(2^1 \times 3^5)$ Taguchi standard

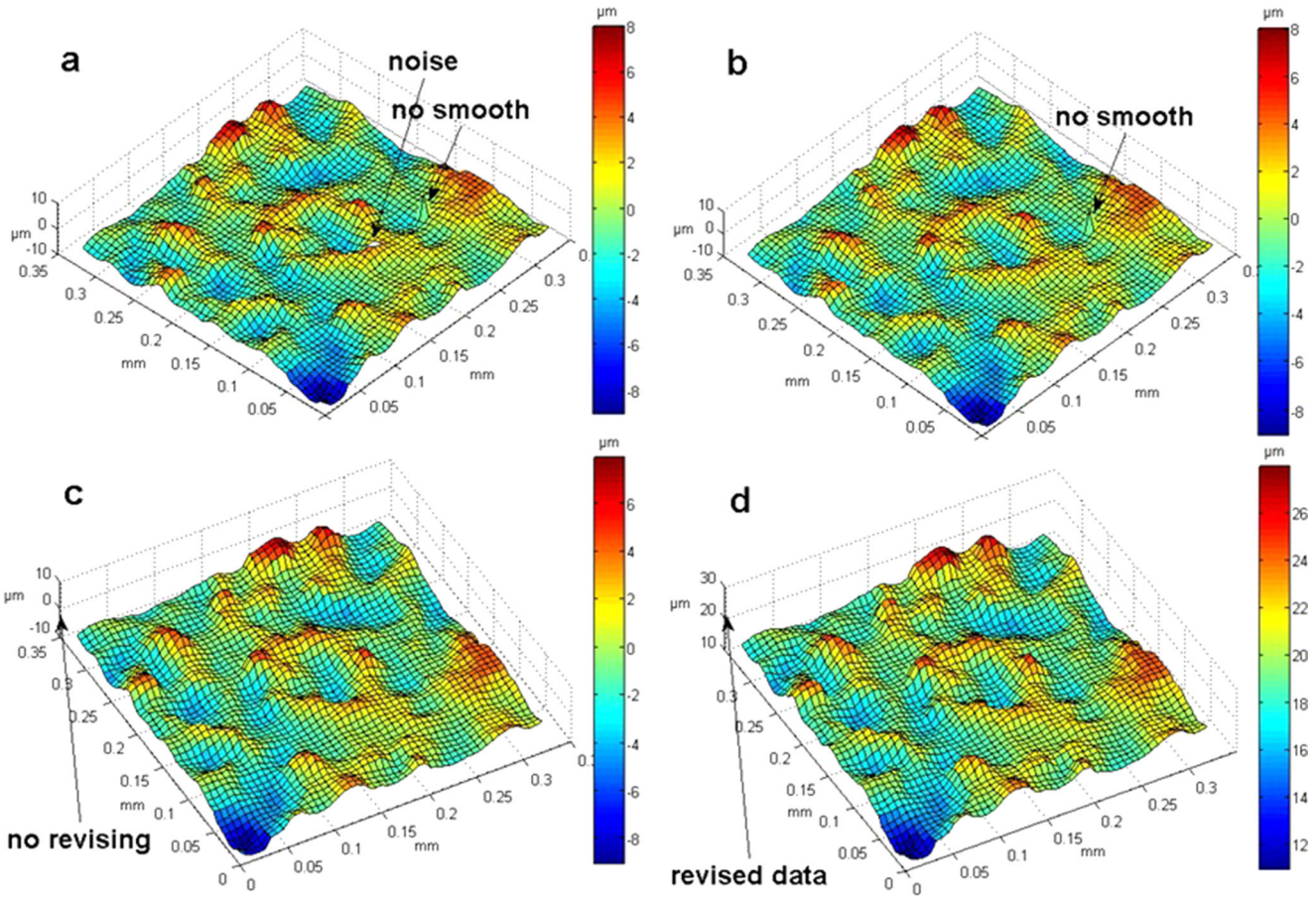


**Fig. 5** Construction of 3D surface topography: **a** raw data, **d** removing noises, **c** smoothing data, and **d** revising data

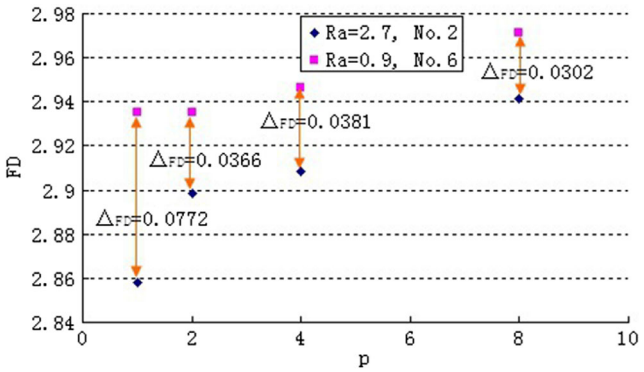


**Fig. 6** FD on the different values of $p$ in two samples

orthogonal array. It is noted that the run orders of all 18 experiments are selected randomly. Figure 7 shows the 3D micron-scale surface topography for typical four WEDM samples.

In order to obtain the relation between surface roughness and FD, the experiment of 3D micron-scale surface with different roughness is analyzed in this paper. The relation between FD and 3D roughness (Sq) is drawn in Fig. 8. FD generally descends with the increment of surface roughness (Sq), but it is also observed in Fig. 8 that the relation is not strictly consistent. The 3D roughness evaluation parameter Sq is 2.466 and 2.418 μm for the point 8 (experimental no. 8) and 9 (experimental no. 9) in Fig. 8, and the FD is 2.8836 and 2.8707, respectively. As it is mentioned, the value of FD depicts the complicated degree of 3D micron-scale surface. It can be seen from Fig. 7c, d that the surface of experimental no. 8 is smoother than that of experimental no. 9. Therefore, the FD of experimental no. 8 is greater than that of experimental no. 9, whereas the difference of their 3D roughness is very small. As mentioned above, it can be generally seen that there exists a relationship between the 3D micron-scale surface topography and FD. If the 3D roughness (Sq) is higher, then the FD is larger. Contrarily, if the 3D roughness (Sq) is lower, then the FD is smaller. This means that FD can be seen as one of global characterization index on 3D micron-scale surface topography.

## 4.2 Main effect of process parameters

In this research, Minitab 16 statistical software was utilized for data analysis. Figure 9 draws the main effect of factors on FD for WEDM machining. It is noted that the data mean is utilized to determine factor effects. By this figure, the factor effects can be visually observed. Figure 9a illustrates the effect of pulse-on time on FD. It shows that pulse-on time has an extremely important effect on FD. In addition, there is a clear linear relationship in pulse-on time and FD; the FD decreases significantly by

**Table 5** Experimental results on machining

| No. | P.O. | P.F. | C.F. | W.T. | W.S. | W.P. | FD | M.T. |
|---|---|---|---|---|---|---|---|---|
| 1 | 3 | 10 | 1 | 6 | 3 | 5 | 2.9428 | 16.38 |
| 2 | 8 | 10 | 2.5 | 10 | 4 | 5 | 2.8559 | 7.92 |
| 3 | 13 | 10 | 4 | 14 | 6 | 5 | 2.8717 | 3.95 |
| 4 | 8 | 20 | 1 | 6 | 4 | 5 | 2.8666 | 4.97 |
| 5 | 13 | 20 | 2.5 | 10 | 6 | 5 | 2.8748 | 2.02 |
| 6 | 3 | 20 | 4 | 14 | 3 | 5 | 2.9458 | 19.28 |
| 7 | 13 | 35 | 1 | 10 | 3 | 5 | 2.8463 | 5.12 |
| 8 | 3 | 35 | 2.5 | 14 | 4 | 5 | 2.8836 | 36.5 |
| 9 | 8 | 35 | 4 | 6 | 6 | 5 | 2.8707 | 5.17 |
| 10 | 8 | 10 | 1 | 14 | 6 | 11 | 2.8532 | 5.08 |
| 11 | 13 | 10 | 2.5 | 6 | 3 | 11 | 2.8321 | 1.79 |
| 12 | 3 | 10 | 4 | 10 | 4 | 11 | 2.9335 | 17.92 |
| 13 | 3 | 20 | 1 | 10 | 6 | 11 | 2.9319 | 38.7 |
| 14 | 8 | 20 | 2.5 | 14 | 3 | 11 | 2.8581 | 0.97 |
| 15 | 13 | 20 | 4 | 6 | 4 | 11 | 2.839 | 3.08 |
| 16 | 13 | 35 | 1 | 14 | 4 | 11 | 2.8448 | 4.00 |
| 17 | 3 | 35 | 2.5 | 6 | 6 | 11 | 2.9503 | 28.17 |
| 18 | 8 | 35 | 4 | 10 | 3 | 11 | 2.8624 | 4.68 |

*P.O.* plus-on time; *P.F.* plus-off time; *C.F.* cutting feed rate; *W.T.* wire tension; *W.S.* wire speed; *W.P.* water pressure; *M.T.* machining time (minute)

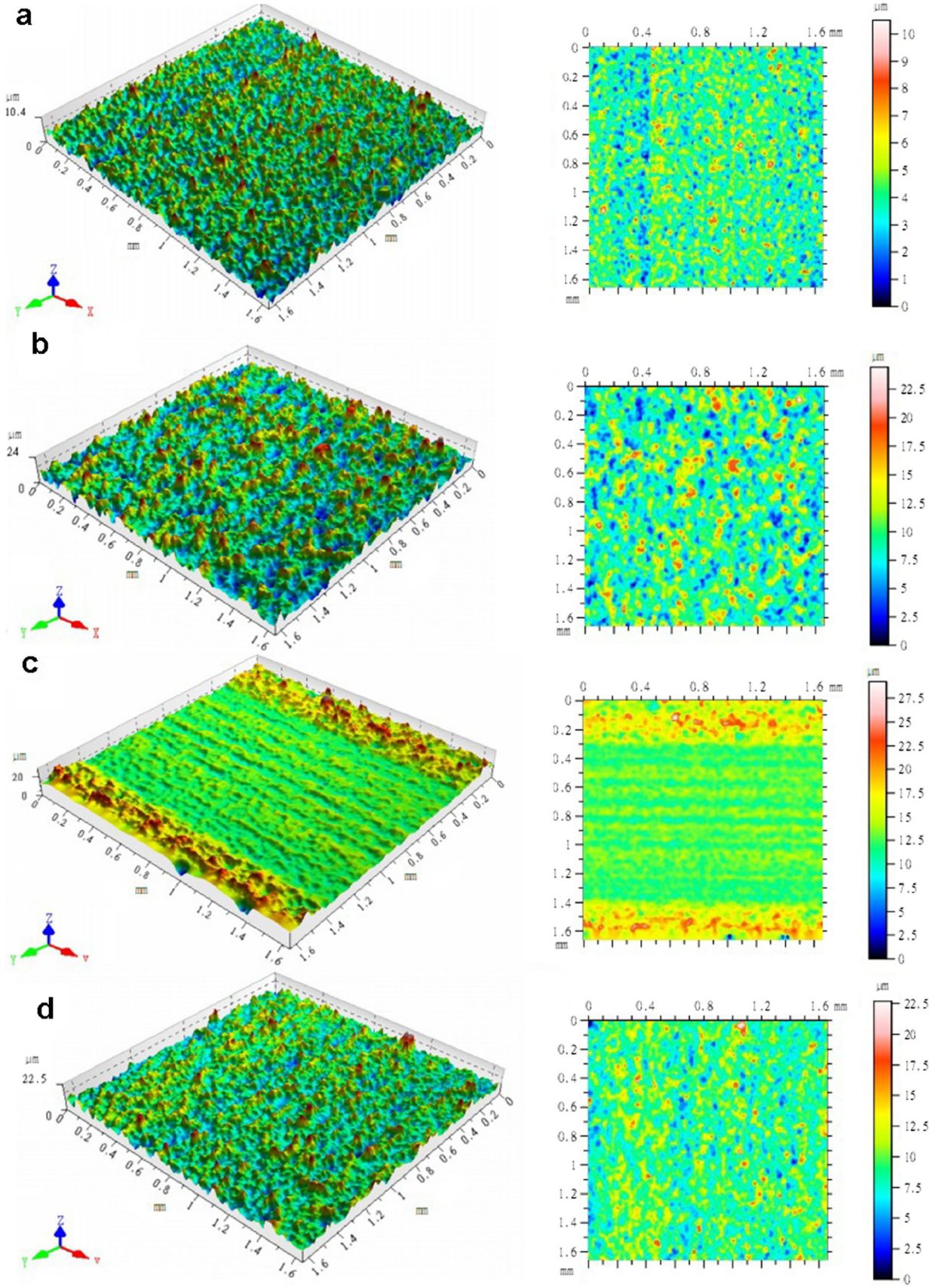


**Fig. 7** 3D micron-scale surface topography of different samples: **a** no. 1, **b** no. 2, **c** no. 8, and **d** no. 9

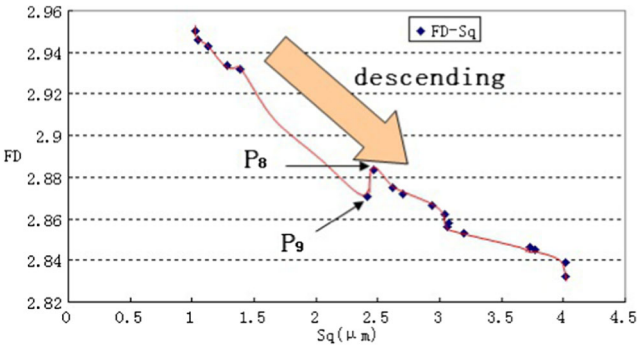


**Fig. 8** The relation between FD and 3D roughness (Sq) of micron-scale surface topography

**Table 6** Main effect of factors on FD

| Factors | Factor effects |
|---|---|
| Pulse-on time (μs) | 0.080 |
| Pulse-off time (μs) | 0.010 |
| Cutting feed rate (mm/min) | 0.011 |
| Wire tension (kgf) | 0.008 |
| Wire speed (m/min) | 0.022 |
| Water pressure (kg/cm$^2$) | 0.006 |

increasing pulse-on time. Figure 9b–f shows the effect of pulse-off time, cutting feed rate, wire tension, wire speed, and water pressure on FD. As it is depicted, none of the factors have an extremely important effect on FD except wire speed and cutting feed rate. The main effect is calculated and shown in Table 6. In statistical analysis, the factor effect is defined as the difference between the two extreme values of the response obtained for the corresponding factor [26].

In addition, the analysis of variance (ANOVA) method was used to analyze the effects of the factors on FD. Minitab 16 was also used for this statistical analysis. The statistically analyzed results for FD is shown in Table 7. DF, Seq SS, Adj SS, and Adj MS are the degree of freedom, the sequential sum of squares, the adjusted sum of squares, and the adjusted mean squares, respectively. $F$ and $P$ represent $F$ value and $P$ value, respectively. In the table, the $F$ of each factor can represent the relative influence of the effect. It is found from Table 7 that the relative influence of pulse-on time is much larger compared to that for the other five factors. The relative influence of the factors on FD is in the following order: pulse-on time $\gg$ wire speed $>$ cutting feed rate $>$ pulse-off time $>$ water pressure $>$ wire tension. Because there are error items of source in Table 7, the relative influence of water pressure is close to that of wire tension. Except the order of the above two factors, that of others is consistent with that in Table 6. Therefore, pulse-on time is the first factor to optimize in the optimization of process parameters, and other almost not significant factors, such as water pressure, could then be set at the economical level. From Fig. 10, it can be seen that the surface craters on experiment no. 11 are much wider and bigger than that on experiment no. 17. These SEM pictures tend to show that the surface produced by the lower pulse-on time, i.e., at 3 μs (see Fig. 10b), is better than that at 13 μs (see Fig. 10a). This finding confirms the 3D surface texture results, whereby the amplitude as well as the FD was found decreased when the pulse-on time was increased from 3 to 13 μs. However, the small craters do not necessarily mean better surface quality. For example, the maximized width and total lengths of crackers on experiment no. 17 are much

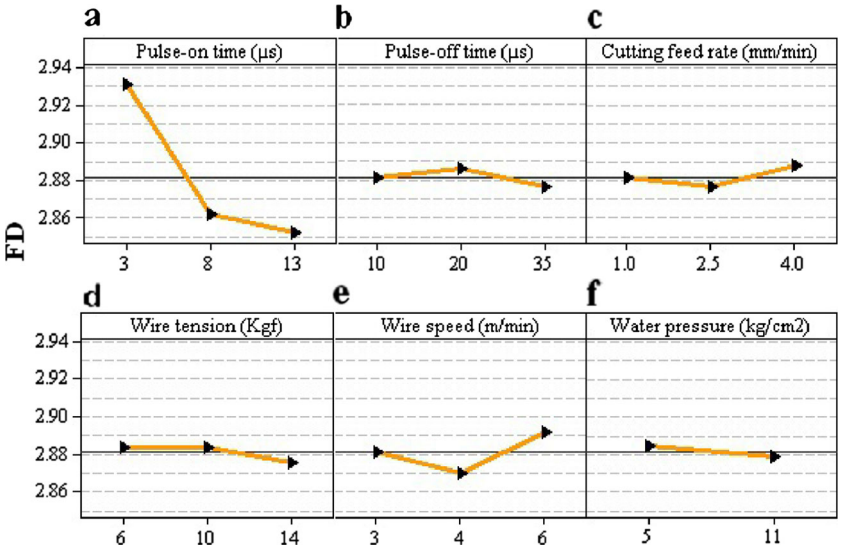


**Fig. 9** Main effect of factors on FD

**Table 7** ANOVA for FD on mean values

| Source | DF | Seq SS | Adj SS | Adj MS | *F* | *P* |
|---|---|---|---|---|---|---|
| Pulse-on time (μs) | 2 | 0.0227923 | 0.0227923 | 0.0113961 | 29.62 | 0.001 |
| Pulse-off time (μs) | 2 | 0.0002818 | 0.0002818 | 0.0001409 | 0.37 | 0.708 |
| Cutting feed rate (mm/min) | 2 | 0.0003900 | 0.0003900 | 0.0001950 | 0.51 | 0.626 |
| Wire tension (kgf) | 2 | 0.0002355 | 0.0002355 | 0.0001178 | 0.31 | 0.747 |
| Wire speed (m/min) | 2 | 0.0013911 | 0.0013911 | 0.0006955 | 1.81 | 0.243 |
| Water pressure (kg/cm$^2$) | 1 | 0.0001555 | 0.0001555 | 0.0001555 | 0.40 | 0.548 |
| Error | 6 | 0.0023082 | 0.0023082 | 0.0003847 | | |
| Total | 17 | 0.0275542 | | | | |

wider and bigger, respectively, than that on experiment no. 11. This is because that the machining time on experiment no. 17 is 15.7 times than that on experiment no. 11, and the flaw might be due to excessive heat focusing on the same microstructure.

### 4.3 Interaction effect of process parameters

The same procedure is used for interaction effect, and Minitab 16 statistical software was also utilized for interaction effect analysis. Figure 11a–c shows the graphs of the FD against pulse-on time for pulse-off time, pulse-on time for wire speed, and cutting feed rate for wire speed, respectively, which are the clear and valuable interaction effect of the prior four important factors for this WEDM. Figure 11a shows the three pulse-off time settings, where the magnitude of FD is maximum at pulse-on time of 3 μs, and also the three graphs are not parallel, thereby indicating that there is an interaction effect between pulse-on time and pulse-off time. For the FD, the trend for the three pulse-off time settings shows that between 3 and 8 μs, there is a rapid effect with a decrease in the height of the peaks, but as pulse-on time increases from 8 to 13 μs, the decline is relatively smooth. For Fig. 11b, also the same trend for the wire speed is observed, with rapid decrease and smoothing decrease at maximum FD of 3 μs. However, there is a general marked increase for wire speed of 6 m/min when pulse-on time exceeds 8 μs. Therefore, this indicates that there is an interaction effect between pulse-on time and wire speed.

It can be drawn from Fig. 11c that the trend of three graphs of wire speed is very different. For the FD, the trend

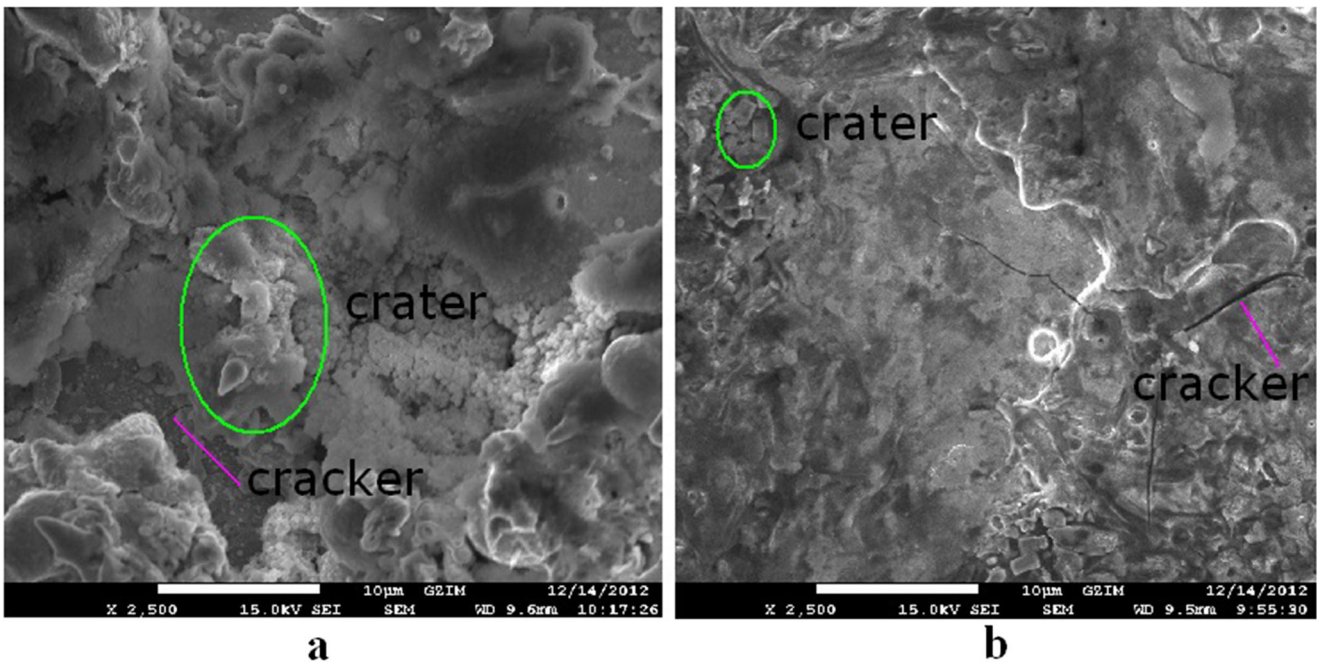


**Fig. 10** SEM pictures of WEDM workpiece: **a** no. 11 and **b** no. 17

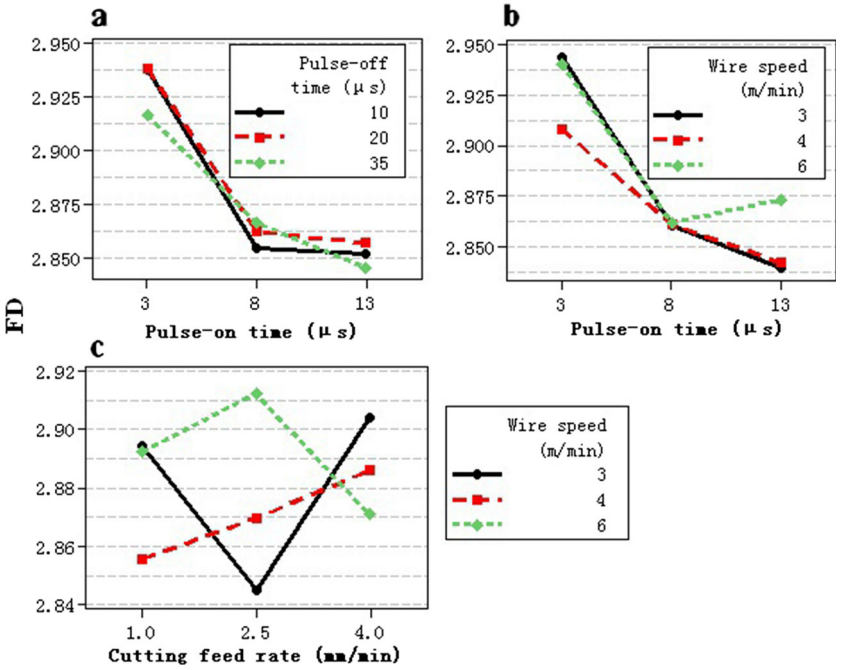


**Fig. 11** Interaction effect of factors on FD

for the wire speed of 3 m/min shows that between 1 to 2.5 mm/min, there is a rapid effect with a decrease in the height of the peaks, but as cutting feed rate is increased from 2.5 to 4 mm/min, there is an increase in them; and the trend for the wire speed of 4 m/min depicts that there is a general marked increase for the cutting feed rate with a maximum FD at 4 mm/min. However, the trend for the wire speed of 6 m/min draws that there is an increase and subsequent decrease with maximum FD amplitude at 2.5 mm/min. It can be drawn from the above analysis that the three graphs are not parallel apparently. Therefore, this indicates that there is an interaction effect between the cutting feed rate and wire speed.

### 4.4 Optimization of process parameters

The characteristic that a larger value represents better machining performance, such as FD and material removal rate, is called the-larger-the-better (LB) [27]. In quality engineering, the S/N ratio (signal-to-noise ratio) could be an effective utilization to obtain the significant parameter from those controlling machining parameters by evaluating the minimum variance. For LB, the definitions of the S/N ratio are listed in Eq. 6:

$$\text{LB}, \eta = -10 \times \log\left(\frac{1}{n}\sum_{i=1}^{n}\frac{1}{y_i^2}\right) \tag{6}$$

in which $\eta$ is the S/N ration, $y_i$ is the response (FD), and $n$ is the number of replications. In this study, the value of $n$ is 1.

The $\eta$ value on FD for machining is presented in Table 8. The largest value of $\eta$ depicts the optimal condition. The optimal settings on FD for machining are listed in Table 9. The next step is to predict and verify the improvement of the performance characteristics. The predicted S/N ratio ($\eta_{\text{opt}}$) which is obtained under the optimal levels of cutting parameters can be calculated as Eq. 7:

$$\eta_{\text{opt}} = \eta_m + \sum_{j=1}^{k}\eta_j - \eta_m \tag{7}$$

where ($\eta_m$) is the total mean of the S/N ratios, ($\eta_j$) is the mean S/N ratio at the optimum levels, and $k$ is the number

**Table 8** $\eta$ value on FD for machining

| Level | Pulse-on time | Pulse-off time | Cutting feed rate | Wire tension | Wire speed | Water pressure |
|---|---|---|---|---|---|---|
| 1 | 56.046 | 55.149 | 55.139 | 55.185 | 55.143 | 82.8 |
| 2 | 54.785 | 55.231 | 55.047 | 55.198 | 54.953 | 82.637 |
| 3 | 54.608 | 55.057 | 55.252 | 55.055 | 55.342 | |
| Delta | 1.438 | 0.174 | 0.205 | 0.143 | 0.199 | 0.163 |

**Table 9** Optimal setting on FD for machining

| Level | Pulse-on time | Pulse-off time | Cutting feed rate | Wire tension | Wire speed | Water pressure |
|---|---|---|---|---|---|---|
| Level number | 1 | 2 | 3 | 2 | 3 | 1 |
| Factor magnitude | 3 | 20 | 4 | 10 | 6 | 5 |

of main design parameters that affect the quality characteristics. The results of the experimental confirmation under the optimal levels of machining parameters are listed in Table 10. It shows the comparison of the predicted FD with the actual FD under the optimal levels of machining parameters for WEDM machining. The improvement in S/N ratio from the initial machining parameters to the level of optimal machining parameters is 0.94 dB. The FD is increased by 11 %.

## 5 Discussion

Contact profilometry is a quantitative technique, which is known to reflect the irregularities of the surface profile of the workpiece. There are a large number of statistical parameters, which can be calculated from the profile data. The most common parameters calculated roughness profile 2D average roughness (Ra), which was developed in the 1950s, and has a long history of experience in the industry; and the most common parameters for three dimensions calculated from roughness profile are the Sq and Sv, which mean the root-mean-square height of surface and the maximum depression height of surface, respectively. However, its physical principles hinder the study of complex objects, such as the fracture surface with overlapping. Standard profilometric methods for assessing roughness for WEDM have produced many estimators derived from height measurements of the surface. Fractal geometry is becoming more and more popular in describing a complex object in biology and materials science, and it is usually used in virtual reality computer program in order to simulate the real world. In this paper, a new graphical evaluation of micron-scale surface topography on WEDM process is proposed by fractal method. The objective is to quantify 3D micron-scale surface topography effect of process parameters on working surface in dressing, as it is analyzed from above that there exists a relationship between the 3D micron-scale surface topography and FD. Generally, if the 3D roughness (Sq) is higher, then the FD is larger; contrarily, if the 3D roughness (Sq) is lower, then the FD is smaller. However, the Sq of experimental no. 8 is larger than that of no. 9, but the FD of experimental no. 8 is bigger than that of no. 9. Therefore, the FD is to obtain markedly different 3D micron-scale surface topography. The surface quality of WEDM is related to the material removal per discharge, which is determined by the pulse energy per discharge. The pulse energy per discharge can be expressed as Eq. 8 as follows:

$$E = \int_0^{t_0} u(t)i(t)dt \tag{8}$$

where $t_0$ is the discharge duration, $u(t)$ is the discharge voltage, $i(t)$ is the discharge current, and $E$ is the pulse energy per discharge. Since the discharge voltage $u(t)$ stays constant during the discharge, the pulse energy per discharge is determined by the pulse duration $t_0$ and discharge current $i(t)$, which is determined by pulse-on time in the WEDM. It can be concluded from the above analysis that pulse-on time has the extremely important effect on FD. In addition, there is a clear linear relationship in pulse-on time and FD; the FD decreases significantly by increasing pulse-on time. Therefore, the pulse-on time is related to the surface quality of WEDM. However, the lower discharge energy do not necessarily mean better surface quality, which can be drawn from SEM, and the too long machine time might be due to excessive heat focusing on the same microstructure in the workpiece of no. 17. WEDM is a thermal process. The mechanical, metallurgical, topological, and chemical conditions of the surface region are described in the surface integrity. Except the main effect of process parameters, they have an interaction effect. The FD against pulse-on

**Table 10** Results of the experimental confirmation on FD

| Initial machining parameters | | Optimal machining parameters | |
|---|---|---|---|
| | | Prediction | Experiment |
| Level | A2B2C2D2E2F2 | A1B2C3D2E3F1 | A1B2C3D2E3F1 |
| FD | 2.8348 | 2.9453 | 2.9468 |
| S/N ratio (dB) | 9.05 | 9.38 | 9.99 |

time for pulse-off time, pulse-on time for wire speed, and cutting feed rate for wire speed, respectively, are the valuable interaction effect for this WEDM. Their trend on FD is very different, which indicates that the thermal process of WEDM is more complicated.

## 6 Conclusion

The effect of machining parameters on 3D micron-scale surface topography in the WEDM of tool steel YG15 related to the fractal dimension is experimentally investigated. The following conclusions are drawn from the present investigation.

1. In this paper, a new graphical evaluation of micron-scale surface topography related to fractal dimension on WEDM process is proposed. The objective is to quantify 3D micron-scale surface topography effect of process parameters on working surface in dressing.
2. There exists a relationship between the 3D micron-scale surface topography and FD. Generally, if the 3D roughness (Sq) is higher, then the FD is larger; contrarily, if the 3D roughness (Sq) is lower, then the FD is smaller.
3. In WEDM, only pulse-on time has the extremely important effect on FD and none of the factors have an extremely important effect on FD expect wire speed and cutting feed rate. But the small craters do not necessarily mean better surface quality from SEM. In addition, there exist interaction effects of the FD against pulse-on time for pulse-off time, pulse-on time for wire speed and cutting feed rate for wire speed, respectively.
4. An optimum parameter combination for the maximum FD is obtained by using the analysis of S/N ratios (see Table 10). The confirmation experiments show that it is possible to increase the FD, which is increased by 11 %.

**Acknowledgments** This research is supported by the National Natural Science Foundation of China (NSFC) under Grant No. 51175207 and Grant No. 51121002. In addition, it is also supported by the National Key Technology R & D Program under Grant No.2012BAF12B00. The key part of BC method is programmed by F. Moisy who comes from University Paris Sud.

## References

1. Rajurkar KP, Pandit SM (1988) Recent progress in electrical discharge machine technology and research. In: Proceedings of Manufacturing International 1988 Atlanta, Georgia, April, Vol 1, pp 219–226
2. Yang YD, Guo JW, Cheng XF, Masanori K (2011) Molecular dynamics simulation of the material removal mechanism in micro-EDM. Precis Eng 35:51–57
3. Qu J, Shih AJ, Scattergood RO (2002) Development of the cylindrical wire electrical discharge machining process, part 2: surface integrity and roundness. ASME J Manuf Sci Eng 124:708–714
4. Liao YS, Woo JC (1997) The effects of machining settings on the behavior of pulse trains in the WEDM process. J Mater Process Technol 71:433–439
5. Gatto A, Iuliano L (1997) Cutting mechanisms and surface features of WED machined metal matrix composites. J Mater Process Technol 65:209–214
6. Aminollah M, Alireza FT, Emanian E, Karimi D (2008) A new approach to surface roughness and roundness improvement in wire electrical discharge turning based on statistical analyses. Int J Adv Manuf Technol 39:64–73
7. Ramakrishnan R, Karunamoorthy L (2004) Surface roughness model for CNC wire electro discharge machining. J Manuf Techol Today 3(5):8–11
8. Mohammadi A, Tehrani AF, Emanian E, Karimi D (2008) Statistical analysis of wire electrical discharge turning on material removal rate. J Mater Process Technol 205:283–289
9. Patowari PK, Saha P, Mishr PK (2011) Taguchi analysis of surface modification technique using W-Cu powder metallurgy sintered tools in EDM and characterization of the deposited layer. Int J Adv Manuf Technol 54:593–04
10. Huang Y, Ming WY, Guo JW, Zhang Z, Liu GD, Li MZ, Zhang GJ (2013) Optimization of cutting conditions of YG15 on rough and finish cutting in WEDM based on statistical analyses. Int J Adv Manuf Technol. doi:10.1007/s00170-013-5037-3
11. Assarzadeh S, Ghoreishi M (2008) Neural-network-based modeling and optimization of the electro-discharge machining process. Int J Adv Manuf Technol 39:488–500
12. Yang RT, Tzeng CJ, Yang YK, Hsieh MH (2012) Optimization of wire electrical discharge machining process parameters for cutting tungsten. Int J Adv Manuf Technol 60:135–147
13. Patowari PK, Saha P, Mishra PK (2010) Artificial neural network model in surface modification by EDM using tungsten copper powder metallurgy sintered electrodes. Int J Adv Manuf Technol 51:627–638
14. Shi HZ, Xie S, Wang X (2013) A warpage optimization method for injection molding using artificial neural network with parametric sampling evaluation strategy. Int J Adv Manuf Technol 65:343–353
15. Razfar MR, Zinati RF, Haghshenas M (2011) Optimum surface roughness prediction in face milling by using neural network and harmony search algorithm. Int J Adv Manuf Technol 52:487–495
16. Ramasawmyam H, Blunt L (2002) 3D surface topography assessment of the effect of different electrolytes during electrochemical polishing of EDM surfaces. Int J Mach Tools Manuf 42:567–574
17. Ramasawmya H, Blunt L (2004) Effect of EDM process parameters on 3D surface topography. J Mater Process Technol 148:155–164
18. Jiang ZD, Wang HR, Fei B (2001) Research into the application of fractal geometry in characterising machined surfaces. Int J Mach Tools Manuf 41:2179–2185
19. Chen MJ, Pang QL, Wang JH, Cheng K (2008) Analysis of 3D microtopography in machined KDP crystal surfaces based on fractal and wavelet methods. Int J Mach Tools Manuf 48:905–913
20. Pentland P (1984) Fractal-based description of natural scenes. IEEE Trans Pattern Anal Mach Intell 6(6):661–674
21. Rimini NR, Maimon O, Romano R (2012) Visual analysis of quality-related manufacturing data using fractal geometry Noa Ruschin-Rimini. J Intell Manuf 23:481–495
22. Eiji U, Takanori K, Hideaki M, Noriaki S (2013) Tissue characterization of coronary plaque by kNN classifier with

fractal-based features of IVUS RF-signal. J Intel Manuf. doi:10.1007/s10845-013-0793-3
23. Mandelbrot BB (1982) The fractal geometry of nature. Freeman, San Francisco
24. Falconer KJ (1990) Fractal geometry mathematical foundation and application. Wiley, New York
25. Russel D, Hanson J, Ott E (1980) Dimension of strange attractors. Phys Rev Lett 45(14):1175–1178
26. Mason RL, Gunt RF, Hess JL (2003) Statistical design and analysis of experiments. Wiley, New York
27. Hicks CR, Turner JK (1999) Fundamental concepts and the design of experiments. Oxford University Press, New York